Sinking CO_2 in supercritical reservoirs

Francesco Parisio[1,†], Victor Vilarrasa[2,3,4*,†]

[1] Chair of Soil Mechanics and Foundation Engineering, Institute of Geotechnics, Technische Universität Bergakademie Freiberg, Germany.

[2] Institute of Environmental Assessment and Water Research (IDAEA), Spanish National Research Council (CSIC), Barcelona, Spain.

[3] Mediterranean Institute for Advanced Studies (IMEDEA), Spanish National Research Council (CSIC), Esporles, Spain.

[4] Associated Unit: Hydrogeology Group UPC-CSIC, Barcelona, Spain.

*Correspondence to: victor.vilarrasa@idaea.csic.es

†The authors equally contributed.

Key points

- We propose a novel geologic carbon storage concept that eliminates CO_2 leakage risk.
- By injecting CO_2 in reservoirs where the resident water stays in supercritical conditions, CO_2 sinks because it is denser than pore water.
- Supercritical reservoirs are found at relatively shallow depths between 3 to 5 km in deep volcanic areas.

Abstract

Geologic carbon storage is required for achieving negative CO_2 emissions to deal with the climate crisis. The classical concept of CO_2 storage consists in injecting CO_2 in geological formations at depths greater than 800 m, where CO_2 becomes a dense fluid, minimizing storage volume. Yet, CO_2 has a density lower than the resident brine and tends to float, hindering the widespread deployment of geologic carbon storage. Here, we propose for the first time to store CO_2 in supercritical reservoirs to eliminate the CO_2 leakage risk. Supercritical reservoirs are found at drilling-reachable depth in volcanic areas, where high pressure (p>21.8 MPa) and temperature (T>374 ºC) imply CO_2 is denser than water. We estimate that 100 injection wells could eventually provide a CO_2 storage capacity in the range of 50-500 Mt yr^{-1}. Carbon storage in supercritical reservoirs is an appealing alternative to the traditional approach.

Plain Language Summary

Geologic carbon storage, which consists in returning carbon deep underground, should be part of the solution to effectively reach carbon neutrality by the mid of the century to mitigate climate change. CO_2 has been traditionally proposed to be stored in sedimentary rock at depths below 800 m, where CO_2 becomes a dense fluid, minimizing the required storage volume. Nevertheless, CO_2 is lighter than brine in the traditional concept, so a rock with sufficient sealing capacity should be present above the storage formation to prevent leakage. Indeed, one of the main hurdles to deploy geologic carbon storage is the risk of CO_2 leakage. To eliminate this risk, we propose a novel storage concept that consists in injecting CO_2 in reservoirs where the pore water stays in supercritical conditions (pressure and temperature higher than 21.8 MPa and 374 ºC, respectively) because at these conditions, CO_2 becomes denser than water. Consequently, CO_2 sinks, leading to a safe long-term storage. This concept, which could store a significant portion of the total requirements to decarbonize the economy, should start being implemented in deep volcanic areas, given that supercritical reservoirs are found at relatively shallow depths between 3 to 5 km.

Keywords

Geologic carbon storage, supercritical geothermal systems, CO_2 leakage, buoyancy, CO_2 emissions reduction.

1. Introduction

Carbon Capture and Storage (CCS) is envisioned as a key technology to accomplish net negative carbon dioxide (CO_2) emissions during the second half of the century and meet the COP21 Paris Agreement targets on climate change (IPCC, 2018; Bui et al., 2018). However, CCS should overcome two main hurdles, namely the risks of induced seismicity (Zoback & Gorelick, 2012; Vilarrasa & Carrera, 2015) and CO_2 leakage (Lewicki et al., 2007; Nordbotten et al., 2008; Romanak et al., 2012), before its widespread deployment takes place. On the one hand, proper site characterization, monitoring and pressure management should allow minimizing the risk of perceivable induced seismicity in Gt-scale CO_2 injection (Rutqvist et al., 2016; Celia, 2017; Vilarrasa et al., 2019). On the other hand, the considered storage formations to date include deep saline aquifers, depleted oil and gas fields and unmineable coal seams in which CO_2 stays in supercritical conditions with a relatively high density, but lower than the one of the resident brine (Hitchon et al., 1999). Thus, the risk of CO_2 leakage remains during hundreds of thousands of years until all CO_2 becomes dissolved into the resident brine or mineralized (Benson & Cole, 2008).

Several concepts have been proposed to date to eliminate the risk of CO_2 leakage. These concepts consist in promoting fast mineralization or storing CO_2 already dissolved in the resident brine. Regarding rapid CO_2 mineralization, injecting CO_2 in shallow basaltic rock allows a quick mineralization thanks to the favorable chemical composition of the host rock, although leakage through buoyancy remains one major concern in the absence of low-permeable caprocks (Gislason & Oelkers, 2014). Another storage rock for mineralization could be peridotite, in which carbonation occurs naturally when exposed to atmospheric CO_2 (Kelemen & Matter, 2008). Despite peridotite is scarcely available at shallow depths, this rock is estimated to provide a total CO_2 storage capacity in the order of Gt, but the rock would need to be massively hydraulically fractured to reach all the available mineral (Kelemen & Matter, 2008). As far as storage of dissolved CO_2 is concerned, the leakage risk is eliminated because brine is heavier when it is CO_2-saturated (Burton & Bryant, 2009; Sigfusson et al., 2015). CO_2 dissolution can be performed either on surface (Burton & Bryant, 2009) or at the reservoir depth (Pool et al., 2013). To balance the injection and pumping energetic cost, geothermal heat can be recovered and electricity could be produced, provided the temperature is high enough (Pool et al., 2013). However, this storage concept has the drawback that CO_2 injection capacity is limited by CO_2 solubility into the brine, which is around 4 % at reservoirs with 60 ºC (Pool et al., 2013). Such solubility leads to a storage of roughly 0.1 Mt of CO_2 per year and per doublet for a circulating brine flow rate of 80 l s^{-1}, i.e., 2.5 Mt yr^{-1} of water being pumped and re-injected. Thus, very large volumes of brine would need to be circulated – a scenario that makes injection of dissolved CO_2 only feasible for small-scale decentralized CO_2 storage. Overall, the alternatives that have been proposed to eliminate the risk of CO_2 leakage entail a limited storage capacity per well with respect to conventional CO_2 injection in free-phase, which diminishes their attractiveness.

To overcome this limitation, we propose an innovative CO_2 storage concept that eliminates the CO_2 leakage risk, while maintaining a high storage capacity per well, which consists in storing CO_2 in free-phase into supercritical reservoirs. Supercritical reservoirs are found in the deeper part of volcanic areas (depth > 3 km), where high pressure (p>21.8 MPa) and temperature (T>374 ºC) bring the pore water to its supercritical state. At such conditions, an interesting situation occurs: CO_2 density is higher than the one of supercritical water and thus, sinks. Consequently, a low-permeable caprock is not needed in deep volcanic areas. Injecting CO_2 into deeper and hotter reservoirs is a new concept that we propose and we deem feasible in the light of the recent achievements demonstrated at the IDDP-2 project, in which a 4.5 km deep well has been drilled in the Reykjanes volcanic area, Iceland, reaching supercritical water conditions (Friðleifsson et al., 2017).

We examine the potential of storing CO_2 in deep volcanic areas where resident water is in supercritical state. First, we analyze the plausible injection conditions at the wellhead that permit injecting CO_2 with a reasonable compression cost. Next, we explore the CO_2 sinking potential and quantify the CO_2 plume shape and injectivity. Finally, we estimate the injection rates that could be achieved and discuss the worldwide CO_2 storage potential in deep volcanic areas.

2. Materials and methods

2.1. Water and CO_2 equation of state

The equation of state (EOS) of water and CO_2 are computed via the C++ library CoolProp (Bell et al., 2014), available at http://www.coolprop.org/. CoolProp employs the Span and Wagner (1996) EOS of CO_2, which is valid up to 800 MPa pressure and 1100 K temperature, and the Scalabrin et al. (2006) viscosity model. The EOS of water is valid up to 1 GPa of pressure and 2000 K temperature and is taken after Wagner and Pruß (2002), which is based on the IAPWS Formulation 1995. The viscosity of water is taken after Huber et al. (2009).

2.2. Temperature, pressure and density profiles along the wellbore

We have implemented an explicit scheme to compute the fluid properties variation with depth along the wellbore. During CO_2 injection, the cold fluid quenches the well in a relatively short time (days to months), so that at equilibrium a colder annulus forms around the well, hindering heat transfer from the surrounding rock, and the injection process becomes adiabatic (Pruess, 2006). The enthalpy is fixed at corresponding wellhead conditions of pressure and temperature $h(z_0) = f\left(p(z_0), T(z_0)\right)$ and CO_2 density is evaluated with CoolProp functions along the discretized ($n = 1000$ intervals) wellbore depth as a function of temperature and pressure $\rho(z_i) = f\left(p(z_i), T(z_i)\right)$. At each depth increment $i+1$, the pressure increase is given by $p(z_{i+1}) = p(z_i) + g\rho(z_i)(z_{i+1} - z_i)$, where g is gravity acceleration, and $T(z_{i+1} - z_i)$ is calculated assuming constant enthalpy $h(z_i) = h(z_0)$.

To compute the initial reservoir in-situ conditions of the resident water, the weight of the water column to the corresponding depth is calculated assuming thermal equilibrium with the geothermal gradient, hence the only difference with the described procedure is that $T(z_i)$ is known a priori.

2.3. CO_2 plume calculations

We use both analytical and numerical solutions to compute CO_2 injectivity and the plume geometry. For the analytical solution, we use the Dentz and Tartakowsky (2009) solution with the correction to incorporate CO_2 compressibility effects of Vilarrasa et al. (2010). We assume initial pressure and temperature of 34 MPa and 500 °C, respectively, and a pressure buildup at the wellbore of 10 MPa in isothermal conditions. The analytical solution is valid for a confined aquifer scenario, which we have assumed to be 500 m or 1000 m thick. The hypothesis of a confined aquifer represents a lower bound case in terms of injection rate: the structural geology features at depth in volcanic areas are quite uncertain and the presence of low-permeability structures could be represented by faults, chemically altered layers or magmatic intrusions, but could not be present as well.

We numerically solve non-isothermal CO_2 injection in a deep volcanic area using the finite element code CODE_BRIGHT (Olivella et al., 1996), which was extended to simulate non-isothermal CO_2 injection (Vilarrasa et al., 2013). Mass conservation of each phase and energy balance are solved simultaneously. Mass conservation of both CO_2 and water can be written as (Bear, 1972),

$$\frac{\partial(\varphi S_\alpha \rho_\alpha)}{\partial t} + \nabla \cdot (\rho_\alpha \mathbf{q}_\alpha) = r_\alpha, \qquad \alpha = c, w \tag{1}$$

where φ [-] is porosity, S_α [-] is saturation of the α -phase, ρ_α [M L^{-3}] is density of the α -phase, t [T] is time, $\mathbf{q}_\alpha$ [L^3 L^{-2} T^{-1}] is the volumetric flux of the α -phase, r_α [M L^{-3} T^{-1}] is the phase change term and α is either CO_2-rich phase, c, or aqueous phase, w. In the numerical simulations, we neglect evaporation of water into CO_2, i.e., $r_w = 0$. The volumetric flux of the α -phase is given by Darcy's law

$$\mathbf{q}_\alpha = -\frac{k k_{r\alpha}}{\mu_\alpha}(\nabla p_\alpha + \rho_\alpha g \nabla z), \qquad \alpha = c, w \tag{2}$$

where k [L^2] is intrinsic permeability, $k_{r\alpha}$ [-] is α -phase relative permeability, μ_α [M L^{-1} T^{-1}] is α -phase viscosity, p_α [M L^{-1} T^{-2}] is α -phase pressure, g [L T^{-2}] is gravity and z [L] is elevation.

Energy conservation, taking into account the non-negligible compressibility of CO_2, can be expressed as (Nield & Bejan, 2006)

$$\frac{\partial\left((1-\varphi)\rho_s h_s + \varphi \rho_w S_w h_w + \varphi \rho_c S_c h_c\right)}{\partial t} - \varphi S_c \frac{D p_c}{D t} + \nabla \cdot \left(-\lambda \nabla T + \rho_w h_w \mathbf{q}_w + \rho_c h_c \mathbf{q}_c\right) = 0 \tag{3}$$

where ρ_s [M L^{-3}] is solid density, h_α [L^2 T^{-2}] is enthalpy of α -phase ($\alpha = c, w, s$ and s stands for solid), λ [M L T^{-3} Θ] is thermal conductivity and T [Θ] is temperature. We assume local thermal equilibrium of all phases at every point.

The liquid density is computed as

$$\rho_w = \rho_{w0} \exp\left(\beta\left(p_w - p_{w0}\right) + \alpha_T T\right)\left(1 + \delta \omega_l^{CO_2}\right), \tag{4}$$

where the reference water density ρ_{w0} equals 1100 kg m^{-3} for the reference pressure $p_{w0} = 0.1$ MPa, water compressibility is $\beta = 4.5\times10^{-4}$ MPa^{-1}, the volumetric thermal expansion coefficient is $\alpha_T = -4.1\times10^{-3}$ K^{-1}, $\delta = 1 - \dfrac{\rho_w V_\phi}{M_{CO_2}}$, $V_\phi = 37.51 - 9.585\times10^{-2}T + 8.740\times10^{-4}T^2 - 5.044\times10^{-7}T^3$ (Garcia, 2003), the molecular mass of CO_2 is $M_{CO_2} = 0.044$ kg mol^{-1}, and $\omega_l^{CO_2}$ is the mass fraction of CO_2 into the liquid phase.

We simulate CO_2 injection into a deep volcanic reservoir with initial temperature and pressure at the top of the injection interval of 500 ºC and 34 MPa, respectively. Unlike the analytical solution (Dentz and Tartakowsky, 2009), the injection interval is not immediately bounded by low-permeable layers. Instead, we inject CO_2 distributed through a vertical well that is open along 500 m centered in a 2 km-thick reservoir that could be either fractured basalt or carbonate rock. The reservoir permeability is 10^{-14} m^2, porosity is 2 %, the retention curve has a gas entry pressure of 0.1 MPa and a van Genuchten shape parameter of 0.5 (Van Genuchten, 1980), relative permeability curves follow cubic functions of the α -phase saturation and the thermal conductivity is 2 W m^{-1} K^{-1}. We prescribe a CO_2 mass flow rate of 1.0 Mt yr^{-1}. CO_2 injection temperature is assumed as 50 ºC, a realistic value given the wellbore calculations (Fig. 1). The outer boundary, placed 5 km away from the injection well, maintains hydrostatic pressure.

The ratio of gravity to viscous forces is given by the gravity number N , defined as (Vilarrasa et al., 2010)

$$N = \frac{2\pi r_{ch} d k \Delta\rho g \rho_{ch}}{\mu_c Q_m}, \tag{5}$$

where for the considered case, $k = 1\times10^{-14}$ m^2, $\Delta\rho$ is the absolute density difference between water and CO_2, $\rho_{ch} = 584.6$ kg m^{-3} is the characteristic density, here assumed as the average CO_2 density between the density in the near field and the far field, r_{ch} is the characteristic length, which is 1 m for the near field and 1000 m for the far field conditions, $d = 500$ m or 1000 m is the aquifer thickness, μ_c is the CO_2 viscosity and Q_m is the mass flow rate of injected CO_2, which equals 4.4 Mt yr^{-1} or 8.7 Mt yr^{-1} for the reservoir thickness of 500 m and 1000 m, respectively. Density and viscosity of water and CO_2 are a function on the pressure and temperature conditions at the near and far field, which are, respectively, $p = 44$ MPa and $T = 50$ °C and $p = 34$ MPa and $T = 500$ °C. The gravity number expresses the relative influence of buoyant forces, taking low values ($N << 1$) when the problem is dominated by the viscous forces and high values ($N >> 1$) when gravity forces dominate.

3. Results

3.1. Injection conditions in the wellbore

CO_2 downhole pressure and temperature conditions are constrained by limiting reservoir cooling and by ensuring an adequate flow rate through sufficient pressure buildup. Assuming wellbore quenching during continuous injection, the injection temperature and pressure at depth depend on the CO_2 wellhead temperature and pressure (Figs. 1 and S1). According to the equation of state (EOS) of CO_2, its density is a function of both temperature and pressure and the adiabatic compression generates an increase in CO_2 temperature with depth (inset in Fig. 1). The density profile, in turn, is responsible for the weight of the fluid column, which translates into a pressure increase with depth (Fig. S1). At 5 MPa of wellhead pressure, the downhole conditions mildly depend on the wellhead temperature. CO_2 is strongly heated up by compression along the wellbore because of its high compressibility as it transitions from gas to supercritical fluid (the critical point of CO_2 is $T = 31.04$ °C and $p = 7.39$ MPa) and reaches the reservoir at approximately 100 °C and $15-17$ MPa, a pressure lower than the one of the reservoir: CO_2 cannot flow into the rock. At a wellhead pressure slightly above the critical pressure (see 7.5 MPa in Fig. 1), the downhole conditions strongly depend upon the wellhead temperature because of phase transition phenomena. While CO_2 is in its supercritical phase when injected warmer than its critical temperature, CO_2 is in liquid phase for cooler injection temperature and reaches the reservoir with higher pressure and lower temperature because of the higher density of the liquid than its gas or supercritical phases. A similar situation occurs when the wellhead pressure equals 10 MPa. At 20 MPa of wellhead pressure, the downhole conditions exhibit small changes between wellhead and downhole temperature because CO_2 density changes are small at such high pressure.

Downhole overpressure is necessary to ensure that CO_2 enters into and flows within the reservoir and, if we assume a reservoir pressure as in IDDP-2 of 34 MPa (Friðleifsson et al., 2017), the downhole pressure should not fall below approximately 40 MPa. For example, to achieve such downhole pressure, the wellhead temperature should not exceed 40 °C for a wellhead pressure of 10 MPa, while CO_2 should be injected at temperature below 30 °C for a wellhead pressure of 7.5 MPa. We can limit reservoir cooling only by injecting at high wellhead pressure and temperature, which implies a high energetic cost.

3.2. CO_2 sinking potential

Above the critical point of water, both fluids are in supercritical phase and CO_2 becomes denser than water at increasingly higher pressure as temperature increases (Fig. 2). The black solid lines in Fig. 2 indicate the pressure and temperature conditions reached by a hydrostatic water column at several depths by taking into account a range of geothermal gradients typical of volcanic areas, indicated with dotted lines. Fig. 2 also shows the CO_2 injection conditions for a wellhead pressure of 10 MPa and several wellhead temperatures along with the estimated in situ conditions of IDDP-2 of 34 MPa and 500 °C (Friðleifsson et al., 2017). For a wellhead pressure of 10 MPa, the maximum wellhead temperature to enable CO_2 injection is approximately 40 °C. At higher wellhead temperature, the CO_2 density along the wellbore is too small to yield a downhole pressure higher than the one of the reservoir. Thermal exchange heats up CO_2 as it flows through the reservoir and CO_2 temperature and pressure equilibrate to the ones of the reservoir at a given distance from the injection point. The starting and end points of the path (yellow line in Fig. 2) in the phase diagram depend upon the reservoir initial conditions and the wellhead injection pressure and temperature. Following our assumptions, the optimum in terms of CO_2 sinking potential corresponds to gradients between 90 and 120 K km^{-1} and at depths >5 km.

3.3. CO_2 plume and injectivity

The analytical solution of Dentz and Tartakowsky (2009) estimates a downward CO_2 plume (Fig. 3a), with the correction of Vilarrasa et al. (2010) applied to consider CO_2 compressibility effects for accurately computing CO_2 density within the plume. We consider a 10-year injection of CO_2 over 500 m and 1000 m-thick reservoirs, assuming a pressure buildup of 10 MPa in a water saturated reservoir initially at $p = 34$ MPa and $T = 500$ °C. The extension and shape of the plume are a function of the reservoir permeability and thickness, with its maximum located in the lower part of the reservoir. The maximum extension of the downward plume spans over almost 2 orders of magnitude for a range of permeability of 3 orders of magnitude, ranging from approximately

2.5×10^{2} m for the less permeable case, to approximately 1.0×10^{4} m for the more permeable one. The achievable mass flow rate is also proportional to the reservoir permeability and thickness and ranges from 0.0057 Mt yr^{-1} to 4.4 Mt yr^{-1} for a 500 m-thick reservoir, and from 0.012 Mt yr^{-1} to 8.7 Mt yr^{-1} for a 1000 m-thick reservoir.

The gravity number N (Eq. (5)), which is the ratio between gravity to viscous forces, is computed for the near field ($T = 50$ °C and $p = 44$ MPa), i.e., close to the injection point, and for the far field ($T = 500$ °C and $p = 34$ MPa), i.e., the initial reservoir conditions. At the near field, water is liquid with $\rho_w = 1006.3$ kg m^{-3} and CO_2 is supercritical with $\rho_c = 940.2$ kg m^{-3}, which yields a $|\Delta\rho| = 66.2$ kg m^{-3} that favors CO_2 buoyancy. At the far field, both fluids are supercritical, with $\rho_w = 138.1$ kg m^{-3} and $\rho_c = 219.2$ kg m^{-3}, which yields a $|\Delta\rho| = 81.0$ kg m^{-3} that favors CO_2 sinking. For a 500 m-thick reservoir, the gravity number is $N = 8.389\times10^{-1} \approx 1$ for the near field and $N = 2.715\times10^{3} >> 1$ for the far field, and for a 1000 m-thick reservoir, $N = 1.678\times10^{0} \approx 1$ for the near field and $N = 5.430\times10^{3} >> 1$ for the far field conditions. According to the gravity number values, at the near wellbore range, viscous forces dominate or are in the range of gravity forces and far enough from the injection point, buoyant forces become predominant (Vilarrasa et al., 2010). Although the near field conditions would favor CO_2 buoyancy, viscous forces are in the same range of buoyant ones and thus, CO_2 buoyancy does not take place or is limited in very thick reservoirs. Far from the injection well, buoyant forces dominate over viscous forces, and since CO_2 has a higher density than water, CO_2 tends to sink (Fig. 4). Finite element analyses of CO_2 injection further confirm that an uprising plume of CO_2 does not develop near the injection well and that CO_2 sinks once it reaches thermal equilibrium with the rock (Fig. 3b and Fig. 4). The CO_2 plume sinks and advances through the bottom of the reservoir. The cooled region concentrates around the injection well (Fig. 3b) and even though CO_2 is lighter than water within this cold region, no upward flow occurs due to buoyancy. Thus, CO_2 sinks, leading to a safe storage despite cooling around the injection well.

4. Discussion

4.1. Challenges

The coupling between the wellbore and the reservoir is important in storage formations with high temperature, like deep volcanic areas. The conflicting objectives of limiting cooling to minimize the risk of inducing seismicity in the long term (Parisio et al., 2019a) and of minimizing compression costs by lowering wellhead pressure can only be resolved with accurate optimization procedures. Since CO_2 density decreases with temperature, the lower the injection temperature, the lower the injection pressure (Fig. 2). Thus, a trade-off arises between the injection pressure and temperature at the wellhead. The optimum injection conditions are site specific and should be computed according to the characteristics of each site. The pressure and temperature injection conditions at the wellhead are coupled to the injectivity of the reservoir and thus, to the required pressure buildup at the downhole to inject a given mass flow rate. Given the highly non-linearity of flow along a wellbore (Lu & Connell, 2014), the wellhead injection conditions will be determined by the injection mass flow rate and the reservoir transmissivity.

Injecting relatively cold CO_2 ($T = 20$ °C) reduces the compression costs because of its higher density (Fig. 2). The most energetically efficient option is to inject CO_2 in liquid state, i.e., $T < 31.04$ °C (Vilarrasa et al., 2013), a solution that bears the consequence of cooling down the rock in the vicinity of the injection well. Cooling-induced thermal stress is inversely proportional to the injection temperature and is likely to enhance injectivity (Yoshioka et al., 2019), but also microseismicity by approaching failure conditions: operators may therefore prefer to inject CO_2 at a relatively high temperature ($40 \div 60$ °C). Heating CO_2 entails large energetic costs (Goodarzi et al., 2015), which in volcanic areas could be minimized by extracting heat from the existing geothermal wells. Injecting hot also increases compression cost because the higher the injection temperature, the higher the required injection pressure. The energy spent to compress the CO_2 should have a renewable source to comply with the objective of reducing CO_2 emissions. Unlike solar, wind or tidal/wave resources, which provide time-fluctuating power output, geothermal energy best fits the purpose of providing a time-constant heat supply required for continuous CO_2 injection.

Combining geothermal energy production with geologic carbon storage is of particular interest to utilize the injected CO_2 and generate a synergy to maximize the cut of CO_2 emissions in volcanic areas. Exploiting a volcanic area for both geothermal and CO_2 storage purposes would foster subsurface characterization, reducing uncertainty and identifying the most suitable areas for both geothermal production and geologic carbon storage. CO_2 could be eventually used as working fluid once the CO_2 plume has grown enough (Randolph & Saar, 2011).

CO_2 flows within the reservoir with two distinct behaviors in the near and the far fields (Fig. 4). In the near field, the injected CO_2 enters into the storage formation at a much lower temperature than the one of the rock, reversing its sinking tendency. Nevertheless, viscous forces dominate the near-well behavior and CO_2 advances like a plug. As CO_2 flows within the reservoir, viscous forces lose strength relative to buoyancy forces, CO_2 is heated up until it reaches the initial reservoir temperature and converts it into the sinking fluid in the far field. In addition to sinking, CO_2 dissolves into the brine (Hassanzadeh et al., 2007) and carbonate mineralizes at higher rates if the host rock is basalt (Gislason & Oelkers, 2014; McGrail et al., 2016). Both CO_2 dissolution and mineral trapping contribute to improve the safety of geologic carbon storage in deep volcanic areas.

4.2. Managing risks

The CO_2 injection rates in deep volcanic areas can be of up to several Mt per year per well (Fig. 3a). The high injection rates induce pressure buildup and cooling that will in turn affect the geomechanical stability of faults and potentially induce seismic events. Pressure buildup is the main triggering mechanism in the short term and cooling dominates in the long term. The latter may limit the lifetime of injection projects if induced earthquakes become too frequent or of excessively high magnitude (Parisio et al., 2019a). The thresholds in frequency and magnitude of induced seismicity is site specific, and depends on the local structural and tectonic features. Thresholds to induced seismicity, both in terms of magnitude and frequency, depend on the local conditions and on the consequences produced on the population and infrastructure: the risk might be low in isolated areas, but unbearably high in densely populated volcanic areas around the world. In any case, induced seismicity risks should be minimized through subsurface characterization, continuous monitoring and adequate pressure and temperature management.

The risks of CO_2 injection in volcanic areas are site-specific, should be carefully assessed and evaluated prior to each potential development project. These risks are connected with the intrinsic risks of active volcanism, namely, CO_2 degassing, hydrothermal explosions and magmatic eruptions-occurrences that could raise concerns about the feasibility of anthropogenic CO_2 injection. CO_2 degassing is naturally present in volcanic areas and usually has its origin at boiling aquifers with superheated steam, which is buoyant (Chiodini et al., 2001). For the injected CO_2 to leak and eventually reach the surface, it should reverse its sinking tendency and become buoyant. However, our proposal only considers injecting CO_2 in supercritical reservoirs, which are placed much deeper and at higher temperature and pressure than boiling aquifers. Hydrothermal explosions are caused by spinodal decomposition from metastable states leading to fast re-equilibration phenomena (Thiery & Mercury, 2009) and the relative risks can be increased by long-term fluid extraction in geothermal reservoir, where the pressure drop could bring the system closer to metastable states. We argue that injecting CO_2 will prevent excessive pressure drawdowns and will help maintain a safe distance in the fluid phase-space from metastable and dangerous states, where explosive fluid demixing is possible. The risks of magmatic eruptions are strongly linked with the volcanic activity of a specific site. Consequently, volcanic centers with recent eruptive manifestation should be avoided as target areas of deep CO_2 injection. Avoiding recently active volcanic centers is seldom restrictive in terms of geographical development because supercritical resident brine can be potentially found at drillable depth in several parts of the world where volcanic manifestations are present (Elders et al., 2014). As an example, the Acoculco Caldera Complex has shown no sign of volcanic activity in the form of eruptions and lava flows since approximately 60,000 years ago (Sosa-Ceballos et al., 2018). Nonetheless, two wells drilled within the Caldera recorded a very high geothermal gradient, with approximately 300 °C at 2 km depth (Calcagno et al., 2018).

The feasibility of this technology is strictly connected to the drilling technology available and to the possibility of reaching pressure and temperature above the critical point of water such that CO_2 would sink. For geothermal gradients of $30\ \mathrm{K\ km^{-1}}$, the critical point of water would be encountered at around $13\ \mathrm{km}$ depth, which is currently beyond the available drilling technology. In volcanic areas, because of the higher geothermal gradients, the critical point of water is located at the accessible depth of $3 \div 4\ \mathrm{km}$ (Friðleifsson et al., 2014). Isolating the lower part of the well through proper casing – a great technological challenge per-se (Kruszewski & Wittig, 2018) – is also necessary to ensure that CO_2 is injected at the proper depth.

4.3. Perspectives of technological development

CO_2 injectivity is controlled by reservoir permeability, which is highly dependent on temperature. For example, fractured granite has a transition permeability (called elasto-plastic), which depends on a threshold mean effective stress, itself a function of temperature (Watanabe et al., 2014a). Above the threshold stress, permeability decreases drastically with increasing mean effective stress. In contrast, fractured basalt is stable until high temperature (> 500 °C) and at 450 °C, the observed permeability depends on stress and ranges from 10^{-17} m^2 to 10^{-16} m^2 for a mean effective confining stress of up to 60 MPa (Watanabe et al., 2014a). The mean effective stress in the crust strongly depends on the rheology (Meyer et al., 2019; Parisio et al., 2019b) and its determination at high depth and temperature remains uncertain. Considering that permeability measurements on laboratory specimens tend to underestimate natural permeability at the geological scale (Neuzil, 1994), and that during drilling of IDDP-2, all circulation fluid was lost (Friðleifsson et al., 2017), we believe that in-situ permeability ranging from 10^{-15} m^2 to 10^{-14} m^2 is possible in the fractured basaltic crust (Hurwitz et al., 2007). Additionally, during injection, the fluid pressure opens up pre-existing fractures, while cooling contracts the surrounding rock, generating an additional fracture aperture: assuming a cubic relationship of transmissivity with fracture aperture (for which fracture permeability is expressed as $k = w^2/12$, where w is the fracture aperture), an increase of the fracture aperture of one order of magnitude implies an increase of the fracture transmissivity of three orders of magnitude. Stimulation techniques have also the potential to achieve higher permeability at depth (Watanabe et al., 2017b; 2019).

We estimate that suitable injection sites will permit an injection rate ranging from 0.5 to 8 Mt yr^{-1} per well (Fig. 3a). We also estimate that some 100 wells drilled worldwide in deep volcanic areas for combined geologic carbon storage and geothermal purposes would provide between 50 to 800 Mt of CO_2 would be stored each year without leakage risk. This amount is higher than what is currently being stored and can represent between 1 and 8 % of the total worldwide storage target, a non-negligible contribution to mitigate climate change effects (IPPC, 2018).

We have compared costs between traditional CCS systems and our proposed solution with or without joint geothermal production. Compression costs are similar for all systems as the transport pipeline delivers CO_2 at the injection site at a pressure of around 10 MPa (Vilarrasa et al., 2013), hence can be neglected. For the comparison, we have assumed a CO_2 market price based on the price of European Union Emissions Trading System as of 11/02/2020, i.e., 22.91 € t^{-1} of CO_2, and a mass injection rate of 2 Mt yr^{-1}. For the traditional CCS system, assuming drilling costs of 2.5 M€ for a 1.5 km-deep well, 1 CO_2 injection well per project and an operational lifetime of 30 years, we estimate a total positive value of 22.9 € t^{-1} of CO_2 stored. For deep volcanic CCS, assuming drilling costs of 30 M€ for each 5 km-deep well, 1 CO_2 injection well and 1 geothermal production well per project and an operational lifetime of 15 years, we estimate a total positive value of 31.9 € t^{-1} of CO_2 stored, which becomes 21.9 € t^{-1} of CO_2 stored if geothermal production is not considered. Combined with enhanced supercritical geothermal energy (Parisio et al., 2019a), geological carbon storage in deep volcanic areas can be a precious contribution to achieve net negative emissions.

5. Conclusions

We show that storing CO_2 into reservoirs in which the resident water is in supercritical state will remove the risk of CO_2 leakage. Even when CO_2 is injected much colder than the reservoir temperature, leading to CO_2 becoming locally buoyant, no buoyant forces arise in the wellbore vicinity and a downward plume of sinking CO_2 develops away from the wellbore. The injectivity per wellbore is relatively high due to supercritical fluid mobility, while overpressure remains low. Continuous injection of CO_2 over a decade is safe, because cooling only affects a radius in the order of tens of meters from the injection wellbore. Over a longer time-span, the expansion of the cooled region could induce buoyant forces that drive upward CO_2 migration and might increase local seismicity as faults and fractures respond to thermal induced strains, limiting project lifetime. Injecting CO_2 in deep volcanic areas is economically more attractive than traditional CCS when combined with supercritical geothermal energy production. Our analyses prove that injecting into reservoirs above the critical point of water would constitute a complementary solution to the problem of significantly reducing CO_2 emissions and would extend the current applicability of geologic carbon storage through the CO_2 sinking effect that prevents leakage to the surface.

Acknowledgments

The authors acknowledge funding from the European Research Council (ERC) under the European Union's Horizon 2020 Research and Innovation Programme through the Starting Grant GEoREST (www.georest.eu), grant agreement No. 801809; F.P. acknowledges funding from the Deutsche Forschungsgemeinschaft (DFG, German Research Foundation) – project number PA 3451/1-1.

Author contributions

F.P. and V.V. equally contributed to the design of the study, the analytical and numerical computations and the writing and editing of the manuscript.

Data and materials availability

The calculations are easily reproducible and described in detail in the materials and methods section. The FEM code for computation of CO_2 injection can be downloaded freely at (https://deca.upc.edu/en/projects/code_bright). The input files for the numerical model can be accessed at the institutional repository Digital.CSIC, which practices FAIR principles: https://digital.csic.es/handle/10261/196740.

Conflicts of interest: There are no conflicts to declare

References

Bear, J. (ed.) (1972). *Dynamics of fluids in porous media*, Elsevier, New York.

Bell, I. H., Wronski, J., Quoilin, S., & Lemort, V. (2014). Pure and pseudo-pure fluid thermophysical property evaluation and the open-source thermophysical property library CoolProp. *Industrial & Engineering Chemistry Research*, *53*(6), 2498-2508.

Benson, S. M., & Cole, D. R. (2008). CO_2 sequestration in deep sedimentary formations. *Elements*, *4*(5), 325-331.

Bui, M., Adjiman, C. S., Bardow, A., Anthony, E. J., Boston, A., Brown, S., ..., & Hallett, J. P. (2018). Carbon capture and storage (CCS): the way forward. *Energy & Environmental Science*, *11*(5), 1062-1176.

Burton, M., & Bryant, S. L. (2009). Surface dissolution: minimizing groundwater impact and leakage risk simultaneously. *Energy Procedia*, *1*(1), 3707-3714.

Calcagno, P., Evanno, G., Trumpy, E., Gutiérrez-Negrín, L.C., Macías, J.L., Carrasco-Núñez, G., & Liotta, D. (2018). Preliminary 3-D geological models of los humeros and Acoculco geothermal fields (Mexico)–H2020 GEMex project, *Advances in Geosciences*, *45*, 321-333.

Celia, M. A. (2017). Geological storage of captured carbon dioxide as a large-scale carbon mitigation option. *Water Resources Research*, *53*(5), 3527-3533.

Chiodini, G., Frondini, F., Cardellini, C., Granieri, D., Marini, L., & Ventura, G. (2001). CO_2 degassing and energy release at Solfatara volcano, Campi Flegrei, Italy. *Journal of Geophysical Research: Solid Earth, 106*(B8), 16213-16221.

Dentz, M., & Tartakovsky, D. M. (2009). Abrupt-interface solution for carbon dioxide injection into porous media. *Transport in Porous Media*, *79*(1), 15-27.

Elders, W.A., Nielson, D., Schiffman, P., & Schriener Jr, A. (2014). Investigating ultra high-enthalpy geothermal systems: a collaborative initiative to promote scientific opportunities. *Scientific Drilling*, *18*(18), 35-35.

Friðleifsson, G. Ó., Elders, W. A., Zierenberg, R. A., Stefánsson, A., Fowler, A. P., Weisenberger, T. B.., ... & Mesfin, K. G. (2017). The Iceland Deep Drilling Project 4.5 km deep well, IDDP-2, in the seawater-recharged Reykjanes geothermal field in SW Iceland has successfully reached its supercritical target. *Scientific Drilling*, *23*, 1-12.

Garcia, J. E. (2003). Fluid dynamics of carbon dioxide disposal into saline aquifers. PhD thesis, University of California, Berkeley.

Gislason, S. R., & Oelkers, E. H. (2014). Carbon storage in basalt. *Science*, *344*(6182), 373-374.

Goodarzi, S., Settari, A., Zoback, M. D., & Keith, D. W. (2015). Optimization of a CO_2 storage project based on thermal, geomechanical and induced fracturing effects. *Journal of Petroleum Science and Engineering*, *134*, 49-59.

Hassanzadeh, H., Pooladi-Darvish, M., & Keith, D. W. (2007). Scaling behavior of convective mixing, with application to geological storage of CO_2. *AIChE Journal*, *53*(5), 1121-1131.

Hitchon, B., Gunter, W. D., Gentzis, T., & Bailey, R. T. (1999). Sedimentary basins and greenhouse gases: a serendipitous association. *Energy Conversion and Management*, *40*(8), 825-843.

Huber, M. L., Perkins, R. A., Laesecke, A., Friend, D. G., Sengers, J.V., Assael, M. J., Metaxa, I. M., Vogel, E., Mareš, R., & Miyagawa, K. (2009). New international formulation for the viscosity of H_2O. *J. Phys. Chem. Ref. Data*, *38*(2), 101–125.

Hurwitz, S., Christiansen, L. B., & Hsieh, P. A. (2007). Hydrothermal fluid flow and deformation in large calderas: Inferences from numerical simulations. *Journal of Geophysical Research: Solid Earth*, *112*(B2).

IPCC, (2018). Summary for Policymakers. In: Global Warming of 1.5°C. An IPCC Special Report on the impacts of global warming of 1.5°C above pre-industrial levels and related global greenhouse gas emission pathways, in the context of strengthening the global response to the threat of climate change, sustainable development, and efforts to eradicate poverty [V. Masson-Delmotte, P. Zhai, H.-O. Pörtner, D. Roberts, J. Skea, P.R. Shukla, A. Pirani, W. Moufouma-Okia, C. Péan, R. Pidcock, S. Connors, J.B.R. Matthews, Y. Chen, X. Zhou, M.I. Gomis, E. Lonnoy, T. Maycock, M. Tignor, and T. Waterfield (eds.)].

Kelemen, P. B., Matter, J. (2008). In situ carbonation of peridotite for CO_2 storage. *Proceedings of the National Academy of Sciences*, *105*(45), 17295-17300

Kruszewski, M., & Wittig, V. (2018). Review of failure modes in supercritical geothermal drilling projects. *Geothermal Energy, 6*(1), 28.

Lewicki, J. L., Birkholzer, J., & Tsang, C. F. (2007). Natural and industrial analogues for leakage of CO_2 from storage reservoirs: identification of features, events, and processes and lessons learned. *Environmental Geology, 52*(3), 457.

Lu, M., & Connell, L. D. (2014). The transient behaviour of CO_2 flow with phase transition in injection wells during geological storage–Application to a case study. *Journal of Petroleum Science and Engineering, 124*, 7-18.

McGrail, B. P., Schaef, H. T., Spane, F. A., Cliff, J. B., Qafoku, O., Horner, J. A., ... & Sullivan, C. E. (2016). Field validation of supercritical CO_2 reactivity with basalts. *Environmental Science & Technology Letters*, *4*(1), 6-10.

Meyer, G.G., Brantut, N., Mitchell, T.M., & Meredith, P.G. (2019) Fault reactivation and strain partitioning across the brittle-ductile transition. *Geology*, *47*(12), 1127-1130.

Neuzil, C. E. (1994). How permeable are clays and shales?. *Water Resources Research, 30*(2), 145-150.

Nield, D. A., & Bejan, A. (2006). *Convection in porous media,* Springer, New York.

Nordbotten, J. M., Kavetski, D., Celia, M. A., & Bachu, S. (2008). Model for CO_2 leakage including multiple geological layers and multiple leaky wells. *Environmental Science & Technology*, *43*(3), 743-749.

Olivella, S., Gens, A., Carrera, J., & Alonso, E. E. (1996). Numerical formulation for a simulator (CODE_BRIGHT) for the coupled analysis of saline media. *Engineering Computations, 13*(7), 87-112.

Parisio, F., Vilarrasa, V., Wang, W., Kolditz, O., & Nagel, T. (2019a). The risks of long-term re-injection in supercritical geothermal systems. *Nature Communications, 10*(1), 4391.

Parisio, F., Vinciguerra, S., Kolditz, O., & Nagel, T. (2019b). The brittle-ductile transition in active volcanoes. *Scientific Reports, 9*(1), 143.

Pool, M., Carrera, J., Vilarrasa, V., Silva, O., & Ayora, C. (2013). Dynamics and design of systems for geological storage of dissolved CO_2. *Advances in Water Resources, 62*, 533-542.

Pruess, K. (2006). Enhanced geothermal systems (EGS) using CO_2 as working fluid—A novel approach for generating renewable energy with simultaneous sequestration of carbon. *Geothermics, 35*(4), 351-367.

Randolph, J. B., & Saar, M. O. (2011). Combining geothermal energy capture with geologic carbon dioxide sequestration. *Geophysical Research Letters, 38*(10), GL047265.

Romanak, K. D., Bennett, P. C., Yang, C., & Hovorka, S. D. (2012). Process-based approach to CO_2 leakage detection by vadose zone gas monitoring at geologic CO_2 storage sites. *Geophysical Research Letters, 39*(15), L15405.

Rutqvist, J., Rinaldi, A. P., Cappa, F., Jeanne, P., Mazzoldi, A., Urpi, L., Guglielmi, Y., & Vilarrasa, V. (2016). Fault activation and induced seismicity in geological carbon storage–Lessons learned from recent modeling studies. *Journal of Rock Mechanics and Geotechnical Engineering, 8*(6), 789-804.

Scalabrin, G., Marchi, P., Finezzo, F., & Span, R. (2006). A reference multiparameter thermal conductivity equation for carbon dioxide with an optimized functional form. *J. Phys. Chem. Ref. Data, 35*(4), 1549–1575.

Sigfusson, B., Gislason, S. R., Matter, J. M., Stute, M., Gunnlaugsson, E., Gunnarsson, I., ... & Wolff-Boenisch, D. (2015). Solving the carbon-dioxide buoyancy challenge: The design and field testing of a dissolved CO_2 injection system. *International Journal of Greenhouse Gas Control, 37*, 213-219.

Span, R., & Wagner, W. (1996). A new equation of state for carbon dioxide covering the fluid region from the triple point temperature to 1100 K at pressures up to 800 MPa. *J. Phys. Chem. Ref. Data, 25*, 1509–1596.

Sosa-Ceballos, G., Macías, J.L., Avellán, D.R., Salazar-Hermenegildo, N., Boijseauneau-López, M.E., & Pérez-Orozco, J.D. (2018). The Acoculco Caldera Complex magmas: Genesis, evolution and relation with the Acoculco geothermal system. *Journal of Volcanology and Geothermal Research, 358*, 288-306.

Thiery, R., & Mercury, L. (2009). Explosive properties of water in volcanic and hydrothermal systems. *Journal of Geophysical Research: Solid Earth*, *114* (B5), B05205.

Van Genuchten, M. T. (1980). A closed-form equation for predicting the hydraulic conductivity of unsaturated soils. *Soil Science Society of America Journal, 44*(5), 892-898.

Vilarrasa, V., Bolster, D., Dentz, M., Olivella, S., & Carrera, J. (2010). Effects of CO_2 compressibility on CO_2 storage in deep saline aquifers. *Transport in Porous Media, 85*(2), 619-639.

Vilarrasa, V., Silva, O., Carrera, J., & Olivella, S. (2013). Liquid CO_2 injection for geological storage in deep saline aquifers. *International Journal of Greenhouse Gas Control, 14*, 84-96.

Vilarrasa, V., & Carrera, J. (2015). Geologic carbon storage is unlikely to trigger large earthquakes and reactivate faults through which CO_2 could leak. *Proc. Natl. Acad. Sci. U.S.A., 112*(19), 5938-5943.

Vilarrasa, V., Carrera, J., Olivella, S., Rutqvist, J., & Laloui, L. (2019). Induced seismicity in geologic carbon storage. *Solid Earth, 10*(3), 871-892.

Wagner, W., & Pruß., A. (2002). The IAPWS Formulation 1995 for the Thermodynamic Properties of Ordinary Water Substance for General and Scientific Use. *J. Phys. Chem. Ref. Data, 31*, 387–535.

Watanabe, N., Numakura, T., Sakaguchi, K., Saishu, H., Okamoto, A., Ingebritsen, S.E., & Tsuchiya, N. (2017a). Potentially exploitable supercritical geothermal resources in the ductile crust. *Nature Geoscience*, *10*(2), 140.

Watanabe, N., Egawa, M., Sakaguchi, K., Ishibashi, T., & Tsuchiya, N. (2017b). Hydraulic fracturing and permeability enhancement in granite from subcritical/brittle to supercritical/ductile conditions. *Geophysical Research Letters, 44*(11), 5468-5475.

Watanabe, N., Sakaguchi, K., Goto, R., Miura, T., Yamane, K., Ishibashi, T., Chen, Y., Komai, T., & Tsuchiya, N. (2019). Cloud-fracture networks as a means of accessing superhot geothermal energy. *Scientific Reports, 9*(1), 939.

Yoshioka, K., Pasikki, R., & Stimac, J. (2019). A long term hydraulic stimulation study conducted at the Salak geothermal field. *Geothermics, 82*, 168-181.

Zoback, M. D., & Gorelick, S. M. (2012). Earthquake triggering and large-scale geologic storage of carbon dioxide. *Proc. Natl. Acad. Sci. U.S.A., 109*(26), 10164-10168.

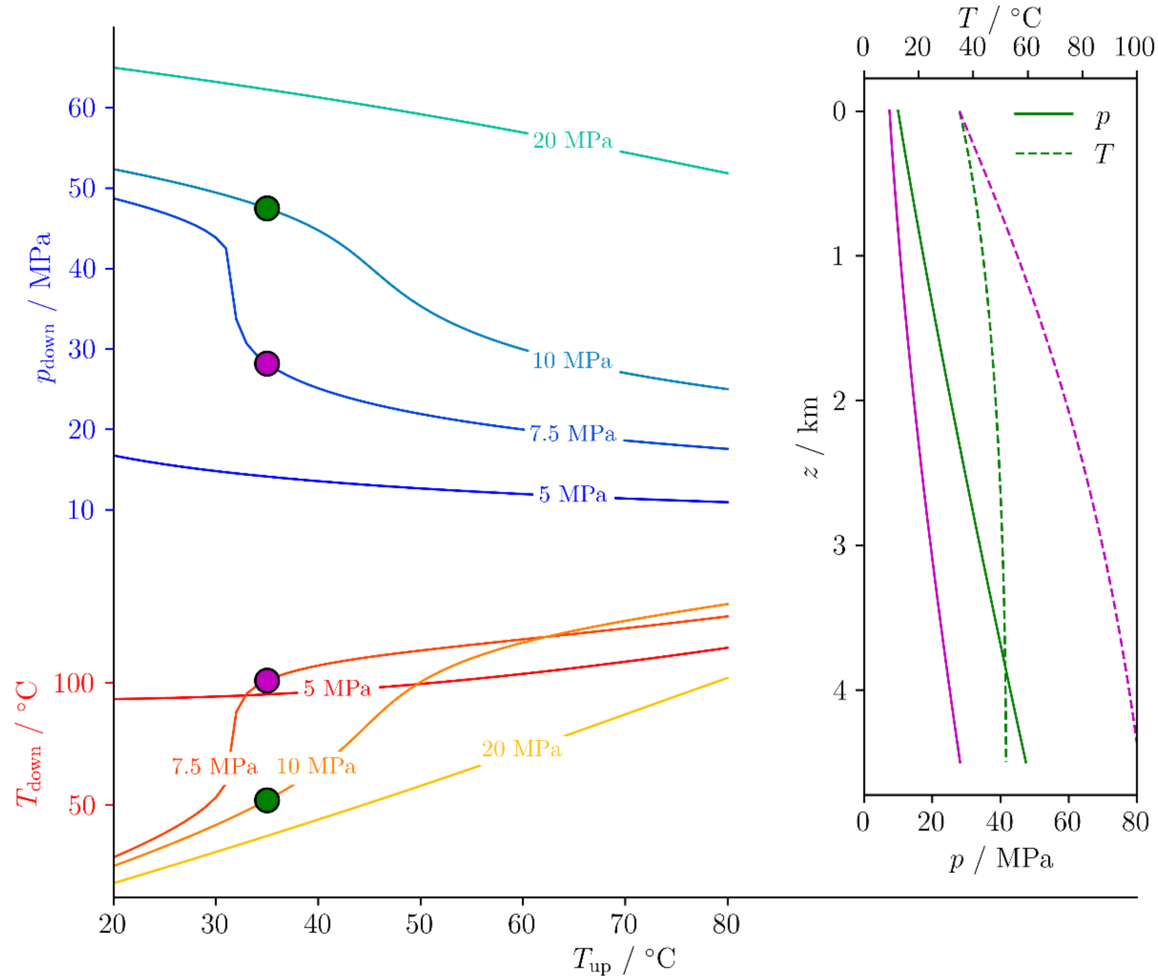

Fig. 1. CO_2 injection conditions at the wellhead and downhole. Each curve shows the pressure, p_{down}, and temperature, T_{down}, conditions at depth of injection (4.5 km) for several wellhead pressures and as a function of wellhead temperature, T_{up}. Injecting CO_2 at a higher wellhead temperature implies that it reaches the reservoir depth with a lower pressure: in order to ensure injectivity into the rock formation, a minimum downhole pressure threshold should be guaranteed and can therefore be achieved by increasing the wellhead pressure. The sharp transition in the curves corresponding to a wellhead pressure of 7.5 MPa is connected to the phase transition from liquid to supercritical close to the critical point, around which abrupt changes in density take place. The inset displays the evolution of CO_2 pressure and temperature along the wellbore depth for two different cases, indicated by points in the main figure (color corresponding to two different

wellhead conditions). Because of the adiabatic hypothesis, the heating of CO_2 is a consequence of pressure increase along the wellbore.

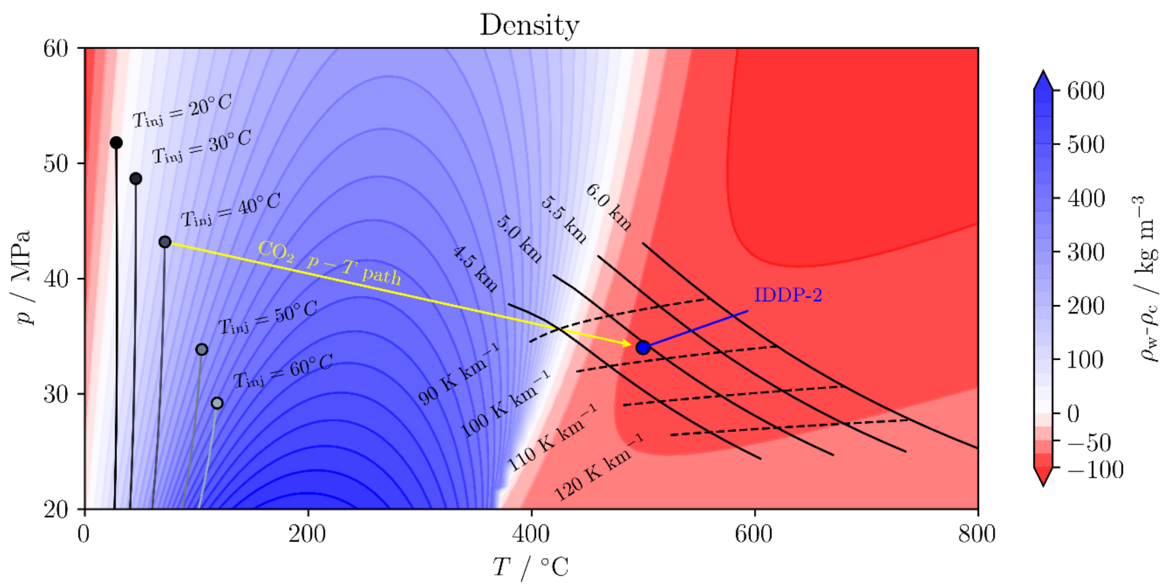

Fig. 2. Density difference map between water and CO_2. The figure shows the density difference between water and CO_2 as a function of pressure (up to 60 MPa) and temperature (up to 800 °C). Positive (in blue) values indicate that CO_2 has a lower density than water, which leads to CO_2 buoyancy, and negative (in red) values indicate that CO_2 has a higher density than water, leading to sinking potential in the reservoir. The downhole conditions of IDDP-2 are temperature of 500 °C and pressure of 34 MPa, which would lead to CO_2 sinking potential. The dotted black lines indicate the $p-T$ conditions of a hydrostatic water column for a variety of geothermal gradients and the solid black lines are iso-depth for the same case. The trajectories on the left-hand side indicate CO_2 injection conditions at the reservoir for several wellhead temperature and for a wellhead pressure of 10 MPa. The yellow line connects the downhole conditions (buoyant) of a hypothetical injection at IDDP2 with the CO_2 conditions (sinking) within the reservoir far from the injection well.

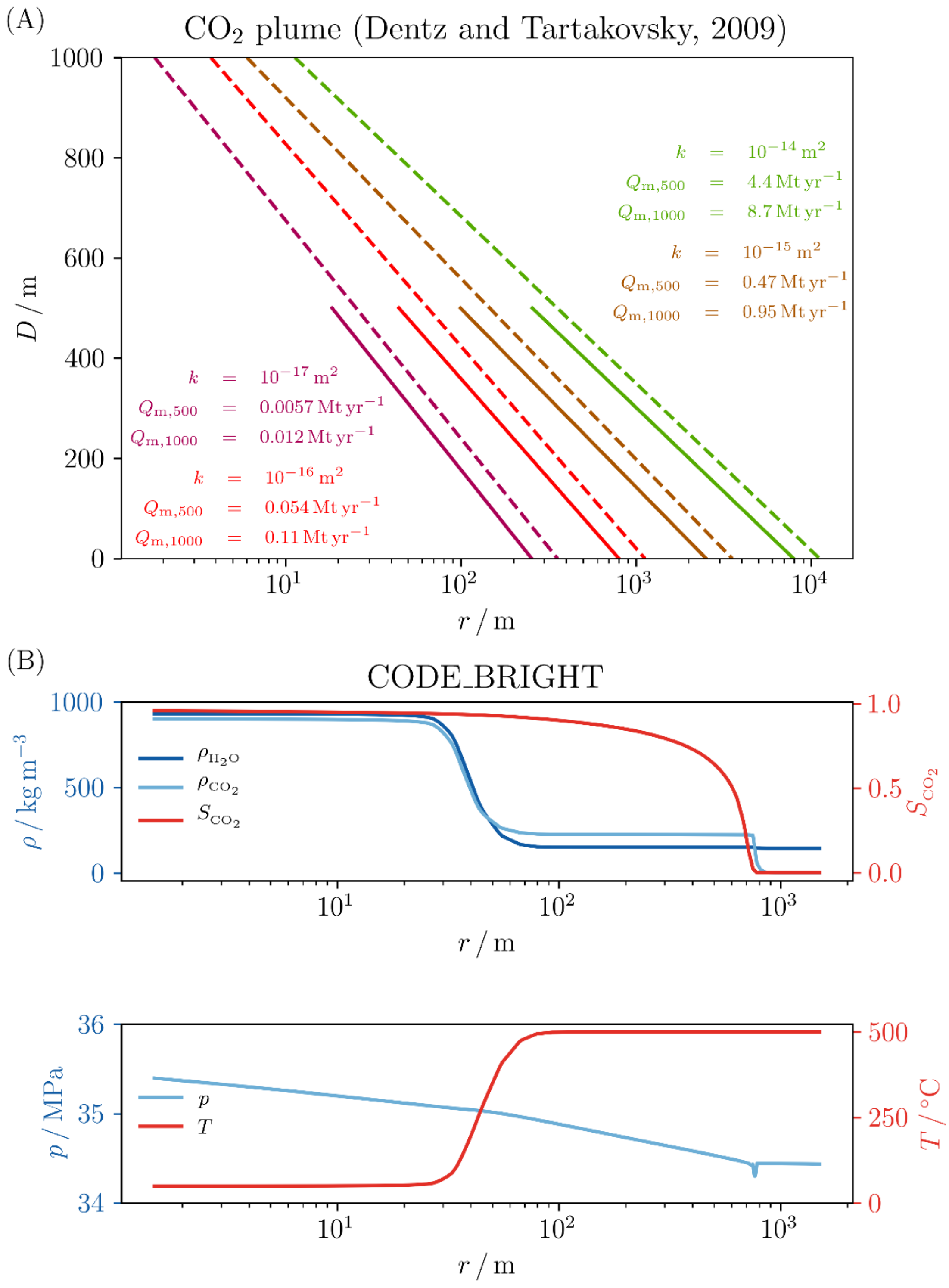

Fig. 3. CO_2 plume. (A) Analytical solutions[15,16] of the CO_2 plume position for a 10-year injection into a 500 m (solid lines) and 1000 m (dotted lines) thick reservoir. We assume a fixed

overpressure of 10 MPa at injection, isothermal injection, an initial reservoir temperature and pressure of 500 °C and 34 MPa, respectively, and a range of reservoir permeability, *k*, that spans three orders of magnitude. The mass flow rate, Q_m, is a function of the reservoir permeability and thickness. The analytical solution predicts a sinking profile due to the density difference between water and CO_2. **(B)** Simulation results after 10 years of injecting 1.0 Mt yr^{-1} of CO_2 at 50 ºC through 500 m of open well centered into a 2000 m-thick reservoir. The extend of the cooled region has a limited size compared to the CO_2 plume and does not affect its sinking tendency.

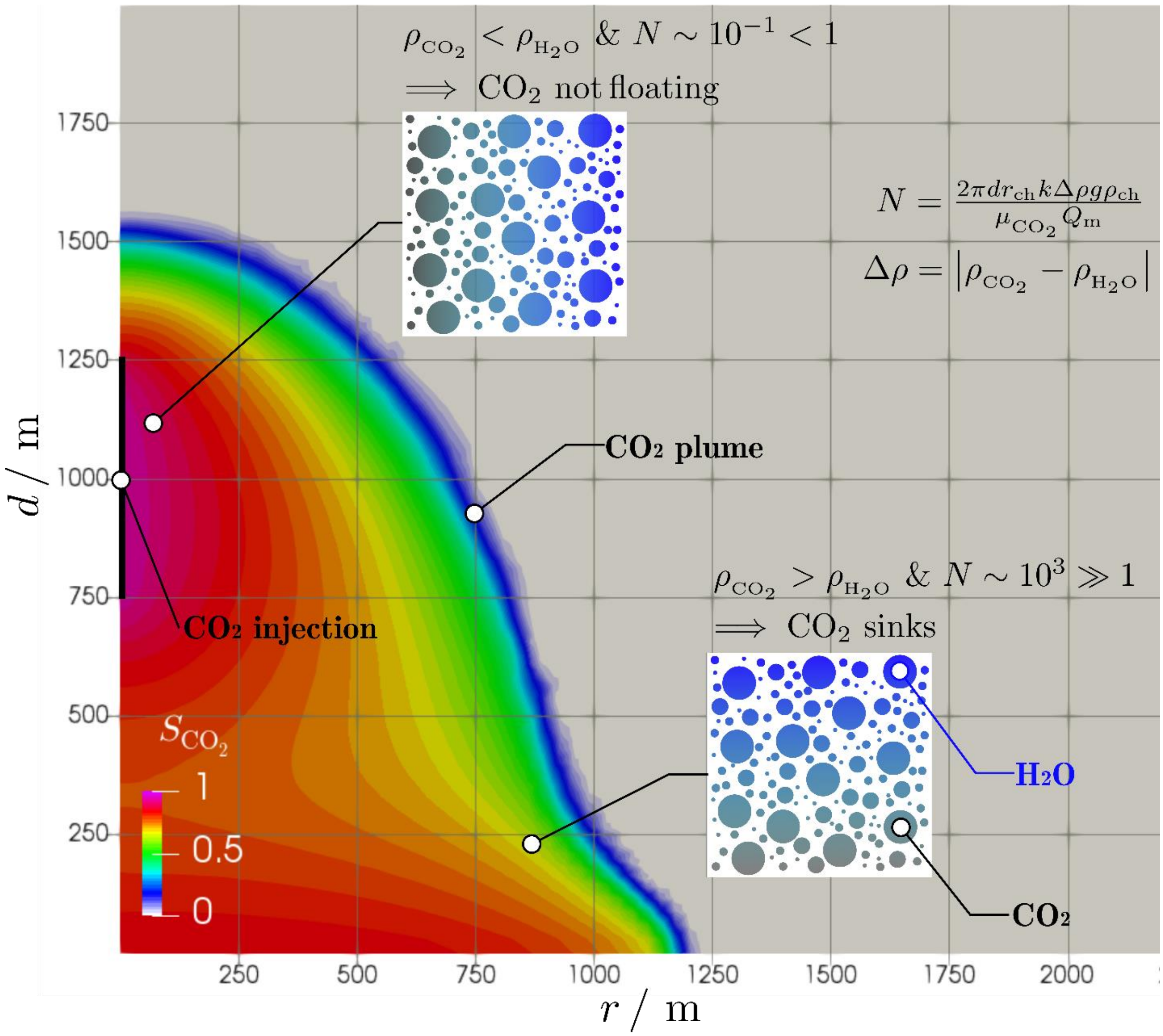

Fig. 4. CO_2 sinking mechanism. The numerically computed sinking profile of CO_2, represented as the area with CO_2 saturation S_c>1, is a consequence of the interplay between gravity and viscous forces as represented by the values of the gravity number N. Cold CO_2 injection does not increase CO_2 buoyant potential because thermal equilibrium is reached within a small region from the wellbore where viscous forces dominate over gravity forces. At the far field, CO_2 is in thermal equilibrium with the reservoir, becoming denser than water, and since gravity forces are greater than viscous ones, CO_2 has the tendency to sink.

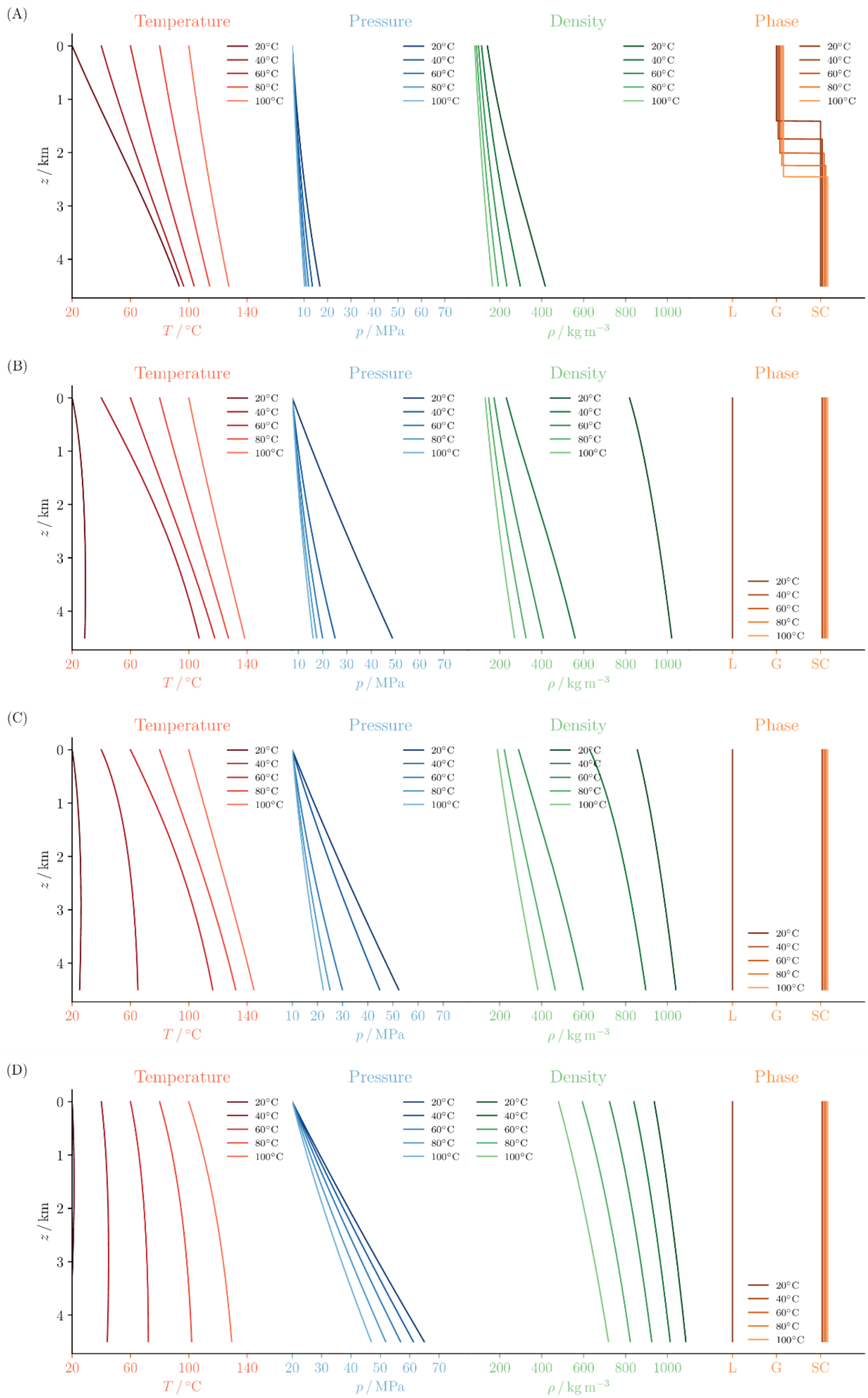
(A)
(B)
(C)
(D)
Temperature
Pressure
Density
Phase
20°C
40°C
60°C
80°C
100°C
z / km
0
1
2
3
4
20
60
100
140
T / °C
10
20
30
40
50
60
70
p / MPa
200
400
600
800
1000
ρ / kg m^{-3}
L
G
SC

Fig. S1. Wellbore path of CO_2 injection. Profile of temperature, pressure, density and phase of CO_2 during isenthalpic injection for a wellhead pressure of (a) 5 MPa, (b) 7.5 MPa, (c) 10 MPa and (d) 20 MPa. The phase curves appear slightly shifted to improve visibility in case of superposition, with symbols indicating liquid (L), gas (G) and supercritical (SC) phase.